

Globular cluster candidates in the Galactic bulge: Gaia and VVV view of the latest discoveries

F. Gran^{1,2}, M. Zoccali^{1,2}, R. Contreras Ramos^{1,2}, E. Valenti^{3,4}, A. Rojas-Arriagada^{1,2},
J. A. Carballo-Bello¹, J. Alonso-García^{6,2}, D. Minniti^{2,5,7}, M. Rejkuba^{3,8}, F. Surot¹

¹ Instituto de Astrofísica, Av. Vicuña Mackenna 4860, Santiago, Chile

² Instituto Milenio de Astrofísica, Santiago, Chile

³ European Southern Observatory, Karl Schwarzschild-Strabe 2, D-85748 Garching bei München, Germany

⁴ Excellence Cluster ORIGINS, Boltzmann-Strasse 2, D-85748 Garching bei München, Germany

⁵ Departamento de Ciencias Físicas, Facultad de Ciencias Exactas, Universidad Andrés Bello, Av. Fernández Concha 700, Las Condes, Santiago, Chile

⁶ Centro de Astronomía (CITEVA), Universidad de Antofagasta, Av. Angamos 601, Antofagasta, Chile

⁷ Vatican Observatory, V00120 Vatican City State, Italy

⁸ Excellence Cluster Universe, Boltzmannstr. 2, 85748 Garching, Germany

Started Aug 2, 2018; Received Dec 27, 2018; Accepted: Apr 14, 2019

ABSTRACT

Context. Thanks to the recent wide-area photometric surveys, the number of star cluster candidates have risen exponentially in the last few years. Most detections, however, are based only on the presence of an overdensity of stars in a given region, or an overdensity of variable stars, regardless of their distance. As candidates, their detection has not been dynamically confirmed. Therefore, it is currently unknown how many, and which ones, of the published candidates, are true clusters, and which ones are chance alignments.

Aims. We present a method to detect and confirm star clusters based on the spatial distribution, coherence in motion and appearance on the color-magnitude diagram. We explain and apply it to one new star cluster, and several candidate star clusters published in the literature.

Methods. The presented method is based on data from the Second Data Release of Gaia complemented with data from the VISTA Variables in the Vía Láctea survey for the innermost bulge regions. It consists of a nearest neighbors algorithm applied simultaneously over spatial coordinates, star color, and proper motions, in order to detect groups of stars that are close in the sky, move coherently and define narrow sequences in the color-magnitude diagram, such as a young main sequence or a red giant branch.

Results. When tested in the bulge area ($-10 < \ell$ (deg) $< +10$; $-10 < b$ (deg) $< +10$) the method successfully recovered several known young and old star clusters. We report here the detection of one new, likely old star cluster, while deferring the others to a forthcoming paper. Additionally, the code has been applied to the position of 93 candidate star clusters published in the literature. As a result, only two of them are confirmed as coherently moving groups of stars at their nominal positions.

Key words. Surveys – Stars: kinematics and dynamics – Galaxy: bulge – globular clusters: general – Proper motions

1. Introduction

Star clusters are invaluable astrophysics tools for a number of reasons. In addition to being a laboratory for stellar evolution, including chemical evolution and self-enrichment, they are among the few objects for which a rather precise age can be measured. If young and massive, their mass function closely resembles the initial mass function (Leigh et al. 2012; Webb & Leigh 2015). For all the others, the radial variation of the present-day mass function allows us to quantify the internal dynamical evolution, while the global present-day mass function is related to the dynamical interaction of the cluster with its environment. Although we do not know exactly how and where massive cluster form (Forbes et al. 2018), we do know that stars do not form in isolation. Most of them form in groups, if not in massive clusters, and therefore the struggle to get a census of the cluster population of a galaxy is motivated by their relevance for the building up of the field star population (Kruijssen et al. 2018).

In the last decades, the number of candidate star clusters reported in the literature has increased significantly, thanks to wide area photometric surveys that allowed to literally scan the sky in

search of groups (Koposov et al. 2007; Belokurov et al. 2010; Muñoz et al. 2012; Ortolani et al. 2012; Belokurov et al. 2014; Laevens et al. 2014; Bechtol et al. 2015; Kim & Jerjen 2015; Laevens et al. 2015b,a; Koposov et al. 2017; Luque et al. 2017; Ryu & Lee 2018, and references therein). Only in the direction of the Galactic bulge, from VISTA Variables in the Vía Láctea (VVV, Minniti et al. 2010) survey images, Minniti et al. (2011) reported the discovery of the candidate globular cluster (GC) VVV-CL001, Moni Bidin et al. (2011) identified two more candidate clusters CL002 and CL003, Borissova et al. (2014) lists 58 new infrared star cluster candidates, and another one, already catalogued as cluster candidate, was further analysed in search for variables by Minniti et al. (2017d). Another 84 old cluster candidates were reported by Minniti et al. (2017c), Minniti et al. (2017a) and Minniti et al. (2017b) based on detection of spatial overdensities, projected overdensities of RR Lyrae variables and projected overdensities of RR Lyrae and type II Cepheids, respectively. Finally, another five globular cluster candidates were identified by Camargo (2018) by visual inspection Wide-field Infrared Survey Explorer (WISE) images.

Although new star clusters can be initially identified as overdensities, the only way to confirm their cluster nature is to verify that their stars move coherently in space, i.e., they are gravitationally bound. This can be done by measuring either radial velocities or proper motions (PMs) of stars in a region centered at the center of the spatial overdensity. In the present paper, we describe a method to identify unusual concentrations of stars simultaneously in the plane of the sky, in the vector point diagram (VPD) and in the color-magnitude diagram (CMD).

The data used here come mostly from the second data release (DR2) of the Gaia mission (Gaia Collaboration et al. 2016; Brown et al. 2018), including positions, PMs (Lindegren et al. 2018) and magnitudes in three photometric bands for all of the stars (Riello et al. 2018; Evans et al. 2018). The work of Pancino et al. (2017), Gaia Collaboration et al. (2018), and Vasiliev (2019) illustrates the potential of Gaia to characterize the globular cluster known up to date. In the region close to the Galactic plane, at latitudes $|b| < 3^\circ$ the Gaia catalogue is highly incomplete due to the large interstellar extinction affecting optical fluxes, and, to a minor extent, to the higher stellar surface density coupled with the limited transmission bandpass of the satellite. In this region, Gaia detects almost exclusively the brightest blue disk stars, while it is virtually blind to the bulge red giants. On the contrary, the near-infrared (near-IR) VVV observations are optimized for the reddest bulge giants, and the PM catalogues obtained with the method described in Contreras Ramos et al. (2017) are both deeper and more precise than the Gaia ones. We use the VVV PMs, in addition to Gaia to analyze candidate clusters at latitudes $|b| < 3^\circ$.

The paper is organized as follows: Sec. 2 describes the automated method to detect –and simultaneously confirm– new star clusters, including the detection of a new old star cluster labelled Gran 1. Sec 3 presents an analysis of the PM of stars within 1 arcmin from the nominal position of a sample of 93 old cluster candidates reported by Minniti et al. (2011); Moni Bidin et al. (2011); Minniti et al. (2017c,a,b); Camargo (2018); Bica et al. (2018). The present clustering method was then applied, with relaxed parameters, within a region of 2 arcmins across the center of each cluster candidate, in order to double check against possible errors in the candidate estimated centers. Finally, Sec. 4 summarizes our results. The VPDs and CMDs of all the unconfirmed candidate clusters are included in the Appendix A.

2. A method to detect coherent groups

The region selected to search for star clusters was the whole bulge area within $-10^\circ \leq (\ell, b) \leq 10^\circ$. This region was divided in small circles of 0.8° radius, centered on every integer degree in Galactic latitude and longitude. An algorithm was developed in order to search for stars that have an unusually large number of neighbors in a 5 dimension phase-space including coordinates, color, and PMs. For each star with complete information, the algorithm counts the number of neighbors within 1 arcmin in space, one mas/yr in PM and 1 mag in color using the K-Dimensional Tree (KDTree) implementation on *scikit-learn* (Pedregosa et al. 2011). For each given field, a minimum threshold of 10 neighbors per star was imposed, in order to ensure statistical significance of the results. Stars with more than 10 neighbors within the complete magnitude range were then searched for groups, in the phase-space mentioned above, with the Density-Based Spatial Clustering of Applications with Noise (DBSCAN) algorithm (Ester et al. 1996) also implemented in the *scikit-learn* package. Groups were kept as *candidate clusters*, and then visually inspected, only if they con-

tained at least 20 members. Note that a group of neighbor stars define “a neighborhood” that may end up being significantly larger than the phase-space radius (1 arcmin, 1 mas yr⁻¹, 1 mag) used for the initial search around each star.

It should be noted that several false positives are detected by the algorithm, close to the mean PM of bulge ($-6, -0.2$) and disk ($-2, -0.5$) field stars, in the VPD. After visual inspection, however, we keep only clusters that define narrow sequences in the CMD, significantly different -by shape and/or tightness- from the main branches of the bulge+disk CMD.

A very first step for the validation of the algorithm described above is that it must be able to rediscover all the clusters known to exist in the area explored. In order to verify this, the catalog of overdensities was cross-matched with the latest version of the Global survey of Milky Way star clusters (MWSC, Kharchenko et al. 2016) catalog in order to identify all the clusters that were previously known. Indeed, we detect all the 45 known bulge globular clusters in this region and $\sim 17\%$ (22/129) of the open clusters up to 5 arcmins from their nominal center. Five known GCs located in the region $|b| < 2.5^\circ$ (Terzan 4, Terzan 6, Terzan 10, 2MASS-GC002 and Djorg 2) were not detected in Gaia, but they were detected in VVV. Another 4 that are listed in the MWSC catalogue as *candidate* GCs, namely ESO 456-09, ESO 373-12, FSR 0019, and FSR 0025, were not detected in any of the two surveys. Based on our data, we do not find any evidence allowing us to confirm their cluster nature.

Figure 1 shows the detection of Terzan 1 ($\ell = -2.44^\circ$, $b = 0.99^\circ$, Ortolani et al. 1999). The mean PM of this cluster is very similar to the mean PM of bulge stars (lower left panel). Nonetheless, the algorithm detects a higher concentration of stars, in the VPD, with respect to a smoother background. Of course, the detection is also triggered by the clustering of Terzan 1 stars both in the plane of the sky (upper left) and in the CMD (right). Note that, as explained above, the algorithm can detect compact sequences of stars, in addition to roundish groups. We overplot here a PGPUC isochrone Valcarce et al. (2013) for a $[\text{Fe}/\text{H}] = -1$ dex, 12 Gyr simple stellar population, at the cluster distance quoted in Kharchenko et al. (2016), in order to confirm that the overdensity is indeed Terzan 1.

The algorithm is also able to detect open star clusters. As an example, Fig. 2 shows the recovery of ESO-589-26, a young star cluster reported at RA=18:02:14 DEC=-21:54:54 (l, b)=($7.9517^\circ, 0.3279^\circ$) that our code independently detected 7 arcsec away from its nominal position. A total of 62 cluster members were identified with our method, defining a narrow main sequence in the CMD and a very coherent group in the VPD. A 3 Myr PARSEC (Marigo et al. 2017) isochrone of solar metallicity is included in the CMD in order to guide the eye. The isochrone was shifted to a distance of ~ 2.4 kpc, as reported in Kharchenko et al. (2016).

Application of this neighbor algorithm to the selected bulge area yielded several cluster candidates not listed in the MWSC catalog. We visually inspected the region within a radius of 5 arcmins from the center of each of them, and end up with at least 7 new globular clusters. The new clusters will be published in dedicated forthcoming papers once they have been spectroscopically confirmed. We show here only one of the new globular clusters, that we name Gran 1, as an example of the ability of the algorithm to find new clusters. Further, we examine the candidate cluster VVV-CL001 (Minniti et al. 2011), VVV-CL002, VVV-CL003 and VVV-CL004 discussed in Moni Bidin et al. (2011), the 84 candidate clusters published in the series of papers by Minniti et al. (2017c), Minniti et al. (2017a) and Minniti

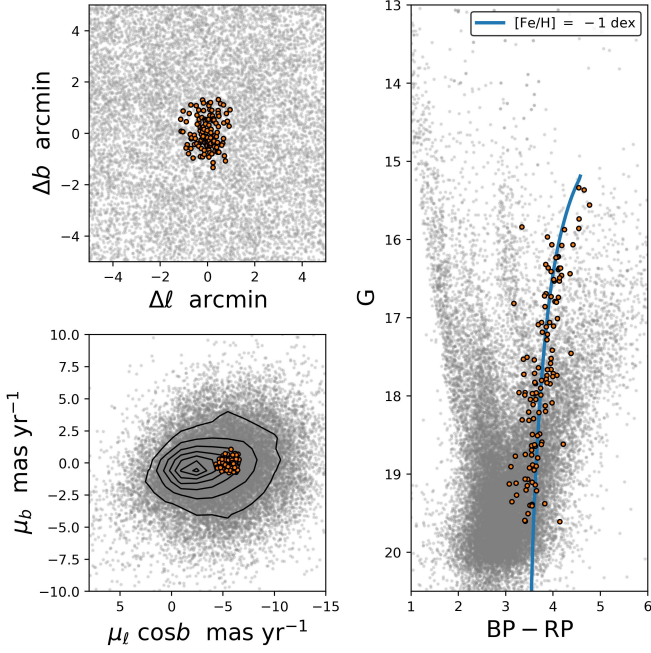


Fig. 1. The globular cluster Terzan 1 as detected by our algorithm. Marked (orange) points represent the detected overdensity along with background stars (gray points) within 15 arcmins from the detected cluster centroid. Gray stars define three populated sequences, from left to right: the disk MS, the disk red clump [both spread along the line of sight] and the bulge upper red giant branch, with a PGPUC isochrone overplotted.

et al. (2017b), plus another 5 candidates presented in Camargo (2018), one of which is further analysed by Bica et al. (2018).

2.1. The new globular cluster Gran 1

A new cluster, not present in the MWSC catalog, was initially detected as a group of 24 stars within 0.731 arcmins from $(\ell, b) = (-1.22^\circ, -3.98^\circ)$ (RA=17:58:36.61 DEC=-32:01:10.72). As we believe that this is the first detection of a cluster in this position, we name it *Gran 1*. The plots that triggered its discovery are shown in Fig. 3. The 24 clustered stars initially found by the code were used to define a cluster center, both in the plane of the sky and in the VPD. These positions were used to select all the stars included both within 2 arcmin in the sky and within 2 mas yr⁻¹ in the VPD, which yielded 95 stars, shown as filled orange circles in Fig. 3. The CMD in the right panel demonstrates that they are compatible with the RGB and horizontal branch (HB) of a cluster with $[\text{Fe}/\text{H}] = -1$ dex, located at a distance of ≈ 8.8 kpc, or $m - M + A_{K_s} = 15$ mag, i.e., within the Galactic bulge. We emphasize that the cluster metal content, distance, and age, cannot be constrained by the present data, as the turnoff cannot be identified in the CMD, future spectroscopic follow-up will derive more precise parameters of this cluster. As a reference, we show a 12 Gyr PGPUC isochrone overplotted to the data, using the putative red clump and HB stars ($J - K_s \sim 0.25$ mag, and $K_s \sim 15$ mag.) as an anchor to estimate a reddening of $E(J - K_s)$ and, adopting the extinction law by Nishiyama et al. (2009), a total extinction of A_{K_s} . The age was assumed to be larger than 10 Gyr, due to the presence of the two blue HB stars, whose nature would need confirmation. If this two stars are proved to be field stars, the age of the candidate cluster could be lower than the estimate we give in Table 1.

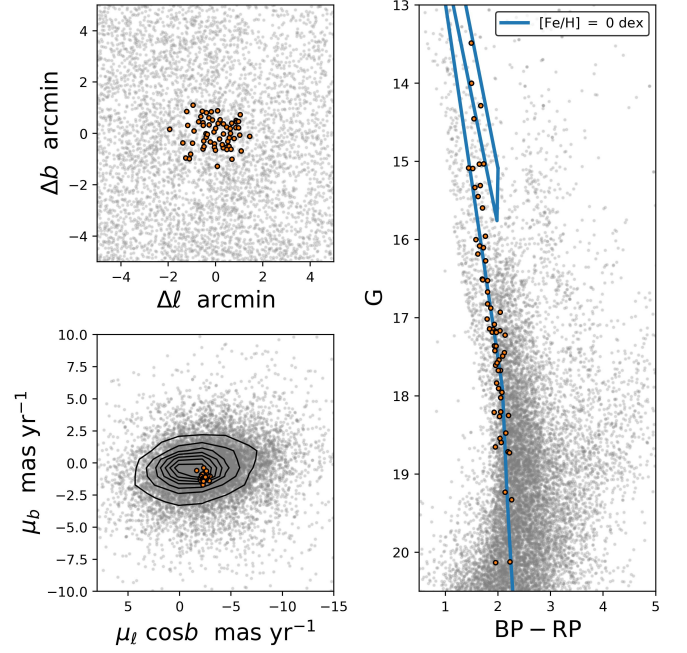


Fig. 2. The open cluster ESO 589-26 as detected by our algorithm. The background sequences are the same as in Fig. 1, although the bulge red giant branch is highly incomplete because this cluster is located very close to the Galactic plane ($b = 0.33^\circ$), in a region of the sky with large interstellar extinction.

Table 1. Basic parameters for the newly discovered GC Gran 1, derived from the present analysis. We emphasize that the metallicity, age and distance for the cluster are very uncertain, as they were derived using 76 stars by comparing the observed CMD with a PGPUC isochrone.

| Parameter | Value | Unit |
|--------------------------|---------------|----------------------|
| ℓ | -1.2320 | deg |
| b | -3.9776 | deg |
| RA (J2015.5) | 17:58:36.61 | hh:mm:ss |
| Dec (J2015.5) | -32:01:10.72 | dd:mm:ss |
| $E(J - K_s)$ | ~ 0.45 | mag |
| A_{K_s} | ~ 0.24 | mag |
| d_\odot | ~ 8.8 | kpc |
| $\mu_\ell \cos b$ | -10.9426 | mas yr ⁻¹ |
| μ_b | 3.0252 | mas yr ⁻¹ |
| $\mu_\alpha \cos \delta$ | -8.0583 | mas yr ⁻¹ |
| μ_δ | -8.0833 | mas yr ⁻¹ |
| Age | $\sim 8 - 12$ | Gyr |
| $[\text{Fe}/\text{H}]$ | ~ -1 | dex |

It should be noted that this cluster would not have been discovered as a high spatial concentration only, as it is an overdensity of only 3.4 sigma above the mean stellar density of the field in this region. It is detected here because the selected cluster member stars are, simultaneously, clustered in the plane of the sky and they share a coherent motion with a median value of $(\mu_\ell \cos b, \mu_b) = (-11, +3)$ mas yr⁻¹, which is off-centered with respect to the mean proper motion of field stars. The integrated magnitude of Gran 1, down to the limit magnitude of the VVV catalogue, is $K_s = 8.07$, while that of Terzan 1, in the same range, is $K_s = 5.24$. Gran 1 is similar in luminosity to Whiting 1, AM 4 or Koposov 1 (Harris 2010). A JYZ color image of the newly discovered cluster is shown in Fig. 4.

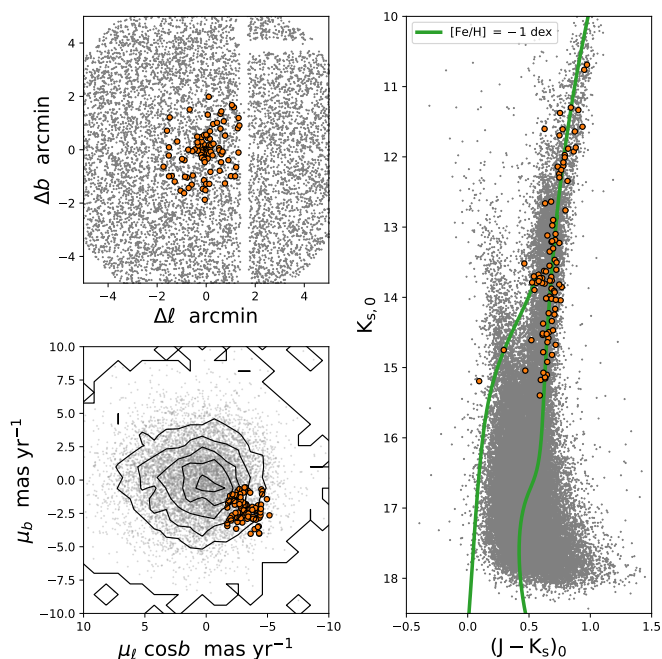


Fig. 3. The new GC Gran 1 as detected in the plane of the sky (upper left), in the VPD (lower left) and in the dereddened CMD (right). All data are from VVV, using the dereddened PSF photometry by Surot et al. (2019) and the PMs from Contreras Ramos et al. (2017). Small, light grey dots are field stars within 5 arcmin from the cluster center given in Table 1, while large orange dots are bona fide cluster members. Blank stripes in the upper left panel denote the chip separations where stars were rejected because the proper motion values were not well constrained (Contreras Ramos et al. 2017).

3. Application to candidate globular clusters in the literature

Hereafter we examine different sets of candidate clusters recently published in the literature. Specifically, Minniti et al. (2011) reported on the discovery of a low mass globular cluster, named VVV GC001, at coordinates $(l, b) = (5.25^\circ, 0.78^\circ)$, (RA=17:54:42.5, DEC=-24:00:53), that is, approximately 10 arcmins away from the known GC UKS 1. On the same year, Moni Bidin et al. (2011) detected three new candidate clusters tentatively named VVV GC002, GC003, and GC004. Upon analysis of their CMD, the same authors concluded that they were most likely a globular cluster, a stellar association, and an overdensity whose nature could not be established, respectively.

In 2017, Minniti et al. compiled a catalog containing 84 GC candidates based on overdensities of stars in the plane of the sky (Minni 1 to Minni 21; Minniti et al. 2017c) and on the coincidence, in the plane of the sky, of a couple or more RRL (Minni 22 to Minni 60; Minniti et al. 2017a) and/or Type II Cepheids (Minni 61 to Minni 84; Minniti et al. 2017b) within 2 arcmins. In the latter two papers, they checked that at least two of the variables within each group had magnitude consistent with similar distances.

Finally, Camargo (2018) published a list of 5 clusters visually selected in multicolor images from the WISE satellite, and then analysed using 2MASS photometry and Gaia DR2 PMs.

The algorithm developed here, applied to the Gaia PM catalog did not blindly detect any of the 93 cluster candidates mentioned above (4 VVV GCs, 84 Minnis, plus 5 Camargos) in the Gaia DR2 catalogue. Because of the much higher stellar density

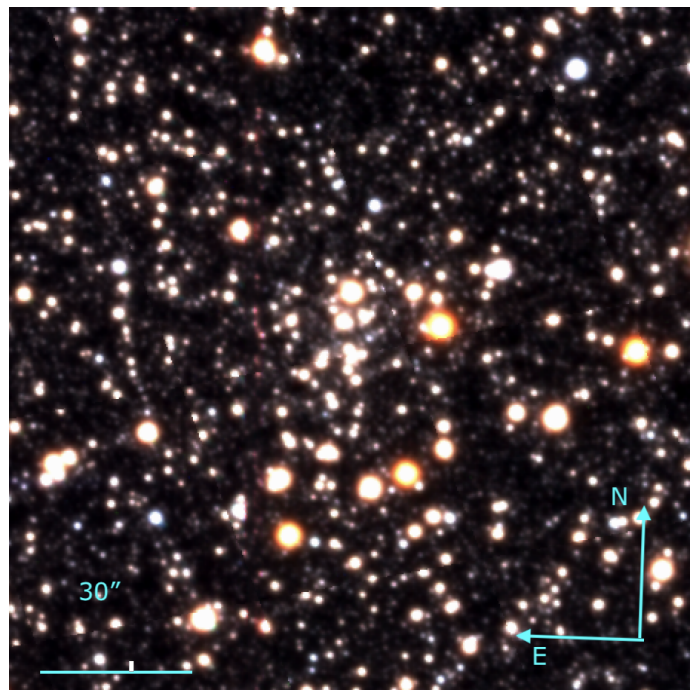


Fig. 4. JYZ Color image of the new GC Gran 1 from the VVV Data Release 4.

close to the plane, a blind search across the VVV area within $|b| \lesssim 3^\circ$ yielded a large number of overdensities, that will be examined and validated in a forthcoming paper. For the present purpose, in order to validate previously published candidate clusters we only need to search in a very restricted area around their nominal centers. Therefore, we have run the original code, this time allowing for a lower minimum number of member stars (15 instead of 20) only in a region of 2 arcmins radius around the candidate centers for stars brighter than $G = 19$ mag. This restricted search was run for all the 93 clusters, on the Gaia catalog, and for the 54 candidates (4 VVV GC, 46 Minnis, and 4 Camargos) within $|b| \lesssim 3^\circ$ on the VVV PM catalog.

As a result, only the candidate VVV GC001 and GC002 seem to be real clusters. Both of them lie relatively close to the plane, and nothing is detected in the Gaia catalog. In VVV data, however, the algorithm picks up an overdensity of stars whose mean PM is offset with respect to the mean PM of field stars, and who define a rather narrower RGB sequence, compared with that of field stars within the same spatial region. This is illustrated in Fig. 5 and Fig. 6.

For all the others, the algorithm either did not detect any overdensity, or it did detect a broad peak, but it was centered, in the VPD, at the same position of the median PM of field stars and the CMD did not show anything different from the CMD of field stars. The Appendix A shows the spatial selection of stars within 1 arcmin from the candidate center, together with their position in the VPD, compared to that of field stars within 10 arcmins of the published center, and the CMD of both. For each cluster, we show these diagrams from Gaia data on the left and, if available, from VVV data on the right. We also include the two confirmed candidates VVV GC001 and VVV GC002 in order to demonstrate that we would have been able to confirm them even without using the clustering algorithm. In fact, by selecting stars within 1 arcmin from their center, in VVV data, the field contamination is larger but a group of stars with mean PM offset from that of field stars is visible in both of them. The offset is smaller

for GC001, where the CMD is better defined, and it is larger in GC002 where the CMD alone would be more ambiguous. On the contrary, by means of these plots, we reject all the clusters were nor the VPD nor the CMD allow seeing anything clearly different from the dominant field population. With this argument, we concluded that, by means of the present data, we cannot confirm the cluster nature of any of the other 91 candidates.

A few considerations are in order. First, it is expected that, by pure Poisson statistics applied to the VPD, one would expect larger fluctuations where the density of stars is higher. That is, at the peak PM of field stars. In other words, we do expect a large number of false positives whose mean PMs is identical to that of the dominant population of field stars, either bulge or disk. Second, we used the catalogue of 150 GC PMs provided by Vasiliev (2019), together with the mean bulge PM from Reid & Brunthaler (2004)¹ to estimate what fraction of known clusters are expected to have a mean PM centered at the mean value for bulge stars. The result is that only 7 clusters have mean PM within 1 mas yr⁻¹ from the mean bulge PM. Of those, only 3 are located within the area explored here, where there are in total 49 clusters. In other words, only 7% of the clusters located in the bulge are expected to have the same mean PM as bulge stars.

If the candidate clusters were massive enough, we would detect them even if their PM would be identical to the peak of bulge stars, as we do for Terzan 1. Therefore, we can safely exclude that any of the 91 candidates that we do not confirm here is as massive as Terzan 1. In order for them to be real, they must have a very low mass, and/or low central concentration *and* their PM must be identical to that of bulge stars. This is expected to be true for at most 6 of them.

4. Summary

We present a clustering algorithm that looks for overdensities simultaneously in a five dimension space including the two coordinates in the sky, the corresponding stellar PMs in each coordinate, and one color. The algorithm was independently applied to the Gaia DR2 catalog of a region of the sky within $-10^\circ \leq (\ell, b) \leq 10^\circ$, and to a VVV catalog including PSF photometry and PMs for stars within $|b| < 3^\circ$, where Gaia is highly incomplete, for bulge stars, due to large interstellar extinction.

With the adopted parameters, discussed in Sec. 2 the algorithm is able to recover all the clusters known to be present in this area, and to find several new young and old star clusters. We presented here the detection of one old cluster named *Gran 1*, and deferred the discussion of the other new clusters to forthcoming, dedicated paper.

The PMs of Gaia and VVV were then used to confirm/dismiss the cluster nature of 93 cluster candidates recently presented in the literature. Based on the requirement that the putative cluster members must move coherently, we could confirm 2 of them (VVV GC001 and GC002) and discarded another 91.

The present result emphasizes that statistical fluctuations of the projected stellar density, in the plane of the sky, or chance alignment of a few variable stars can be relatively frequent, in a huge survey as Gaia and VVV. They can be easily mistaken for a star cluster, because: *i*) the stellar population of the Galactic bulge has a (relatively low) spread in metallicity and age that

¹ The authors quote $(\mu_\ell \cos b, \mu_b) = (-6.379, -0.202)$ mas yr⁻¹ as the absolute PM of Sagittarius A, which must coincide with the mean absolute PM of bulge stars. Converted to equatorial coordinates, it gives $(\mu_\alpha \cos \delta, \mu_\delta) = (-3.15, -5.55)$ mas yr⁻¹, that we subtract from the values in Table B1 from Vasiliev (2019).

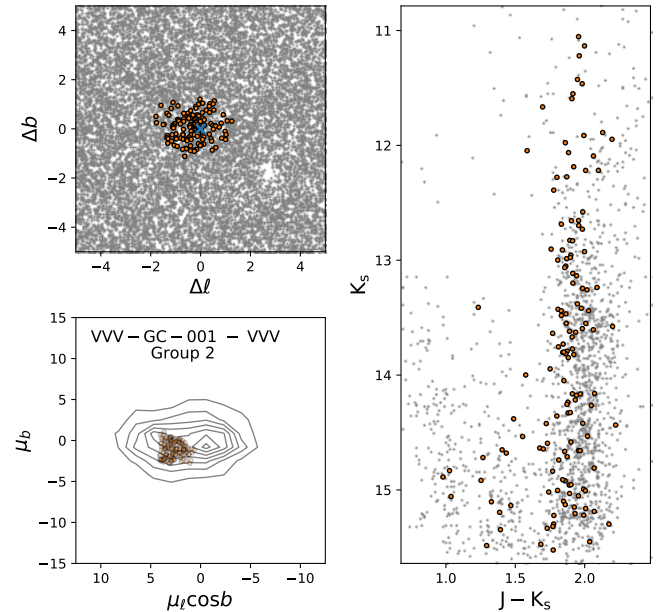


Fig. 5. Diagnostic plots for the globular cluster GC001. Stars within 2 arcmins from the nominal cluster center were used to perform the clustering algorithm. The spatial distribution of stars (Group 2 defined by the code) that comprise the GC are showed in orange points (upper left), plotted the VPD (bottom left) and in the CMD. Note that the distribution of cluster stars is shifted with respect to the contours of the total distribution of stars in the VPD.

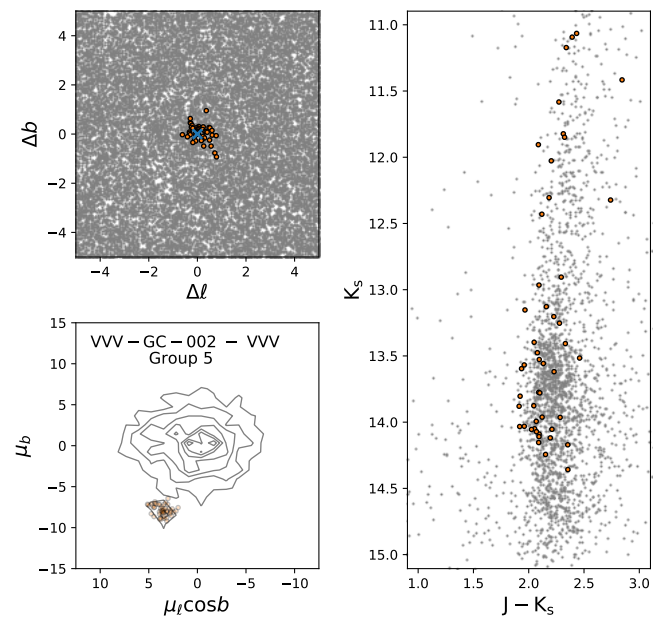


Fig. 6. Same as Fig. 5 for the globular cluster VVV GC002.

makes its RGB only slightly wider than that of a globular cluster; and *ii*) when selecting stars in a small region of the sky, that is within a few arcmins from a spatial overdensity peak, the CMD sequences appear always narrower than those of a wider region, because they are affected by a lower differential extinction. For this reason, the list of candidate new star clusters published in the last few years has increased enormously. Only stellar mo-

tions, however, can confirm the real cluster nature of a detected overdensity and they have proven to dismiss the large majority of candidates. Given the present availability of Gaia PMs across almost the whole sky, claimed detection of new candidate clusters should always be supported by the kinematics analysis, proving that the cluster member stars move coherently in space.

By means of the present data, we cannot exclude that a few of the candidates are extremely low mass clusters that happen to have zero PM with respect to bulge stars, are located at a distance very close to 8 kpc and present relatively broad CMD sequences, possibly due to differential extinction. We can only state that, because of these characteristics, they would be invisible to both Gaia and VVV. It is important to keep this in mind, however, when deciding whether to allocate telescope time to followup studies of such candidates.

Acknowledgements. This work is part of the Ph.D. thesis of F.G., funded by grant CONICYT-PCHA Doctorado Nacional 2017-21171485. F.G. also acknowledge CONICYT-Pasantía Doctoral en el Extranjero 2019-75190166 and ESO SSDF 19/20 (ST) GAR funding. We acknowledge support from the Ministry for the Economy, Development, and Tourism's Programa Iniciativa Científica Milenio through grant IC120009, awarded to Millenium Institute of Astrophysics (MAS), the BASAL CATA Center for Astrophysics and Associated Technologies through grant AFB-170002, and from FONDECYT Regular 1150345. JAC-B acknowledges financial support to CAS-CONICYT 17003.

Based on observations taken within the ESO VISTA Public Survey VVV, Program ID 179.B-2002. This work has made use of data from the European Space Agency (ESA) mission *Gaia* (<https://www.cosmos.esa.int/gaia>), processed by the *Gaia* Data Processing and Analysis Consortium (DPAC, <https://www.cosmos.esa.int/web/gaia/dpac/consortium>). Funding for the DPAC has been provided by national institutions, in particular the institutions participating in the *Gaia* Multilateral Agreement.

This research made use of: TOPCAT (Taylor 2005), GitHub, IPython (Pérez & Granger 2007), numpy (van der Walt & Varoquaux 2011), matplotlib (Hunter 2007), Astropy, a community-developed core Python package for Astronomy (Astropy Collaboration et al. 2013), scikit-learn Pedregosa et al. (2011), galpy: A Python Library for Galactic Dynamics Bovy (2015), and "Aladin sky atlas" developed at CDS, Strasbourg Observatory, France (Bonnarel et al. 2000; Boch & Fernique 2014). This research has made use of NASA's Astrophysics Data System.

References

- Astropy Collaboration, Robitaille, T. P., Tollerud, E. J., et al. 2013, *A&A*, 558, A33
- Bechtol, K., Drlica-Wagner, A., Balbinot, E., et al. 2015, *ApJ*, 807, 50
- Belokurov, V., Irwin, M. J., Koposov, S. E., et al. 2014, *MNRAS*, 441, 2124
- Belokurov, V., Walker, M. G., Evans, N. W., et al. 2010, *ApJ*, 712, L103
- Bica, E., Minniti, D., Bonatto, C., & Hempel, M. 2018, *PASA*, 35, e025
- Boch, T. & Fernique, P. 2014, in *Astronomical Society of the Pacific Conference Series*, Vol. 485, *Astronomical Data Analysis Software and Systems XXIII*, ed. N. Manset & P. Forshay, 277
- Bonnarel, F., Fernique, P., Bienaymé, O., et al. 2000, *A&AS*, 143, 33
- Borissova, J., Chené, A.-N., Ramírez Alegría, S., et al. 2014, *A&A*, 569, A24
- Bovy, J. 2015, *ApJS*, 216, 29
- Brown, A. G. A., Vallenari, A., Prusti, T., et al. 2018, *A&A*, 616, A1
- Camargo, D. 2018, *ApJ*, 860, L27
- Contreras Ramos, R., Zoccali, M., Rojas, F., et al. 2017, *A&A*, 608, A140
- Ester, M., Kriegel, H.-P., Sander, J., & Xu, X. 1996, in (AAAI Press), 226–231
- Evans, D. W., Riello, M., De Angeli, F., et al. 2018, *A&A*, 616, A4
- Forbes, D. A., Bastian, N., Gieles, M., et al. 2018, *Proceedings of the Royal Society of London Series A*, 474, 20170616
- Gaia Collaboration, Helmi, A., van Leeuwen, F., et al. 2018, *A&A*, 616, A12
- Gaia Collaboration, Prusti, T., de Bruijne, J. H. J., et al. 2016, *A&A*, 595, A1
- Harris, W. E. 2010, *ArXiv e-prints*
- Hunter, J. D. 2007, *Computing In Science & Engineering*, 9, 90
- Kharchenko, N. V., Piskunov, A. E., Schilbach, E., Röser, S., & Scholz, R. D. 2016, *A&A*, 585, A101
- Kim, D. & Jerjen, H. 2015, *ApJ*, 799, 73
- Koposov, S., de Jong, J. T. A., Belokurov, V., et al. 2007, *ApJ*, 669, 337
- Koposov, S. E., Belokurov, V., & Torrealba, G. 2017, *MNRAS*, 470, 2702
- Kruijssen, J. M. D., Pfeffer, J. L., Reina-Campos, M., Crain, R. A., & Bastian, N. 2018, *MNRAS*, 1537
- Laevens, B. P. M., Martin, N. F., Bernard, E. J., et al. 2015a, *ApJ*, 813, 44
- Laevens, B. P. M., Martin, N. F., Ibata, R. A., et al. 2015b, *ApJ*, 802, L18
- Laevens, B. P. M., Martin, N. F., Sesar, B., et al. 2014, *ApJ*, 786, L3
- Leigh, N., Umbreit, S., Sills, A., et al. 2012, *MNRAS*, 422, 1592
- Lindegren, L., Hernández, J., Bombrun, A., et al. 2018, *A&A*, 616, A2
- Luque, E., Pieres, A., Santiago, B., et al. 2017, *MNRAS*, 468, 97
- Marigo, P., Girardi, L., Bressan, A., et al. 2017, *ApJ*, 835, 77
- Minniti, D., Alonso-García, J., Braga, V., et al. 2017a, *Research Notes of the American Astronomical Society*, 1, 16
- Minniti, D., Alonso-García, J., & Pullen, J. 2017b, *Research Notes of the American Astronomical Society*, 1, 54
- Minniti, D., Geisler, D., Alonso-García, J., et al. 2017c, *ApJ*, 849, L24
- Minniti, D., Hempel, M., Toledo, I., et al. 2011, *A&A*, 527, A81
- Minniti, D., Lucas, P. W., Emerson, J. P., et al. 2010, *New A*, 15, 433
- Minniti, D., Palma, T., Dékány, I., et al. 2017d, *ApJ*, 838, L14
- Moni Bidin, C., Mauro, F., Geisler, D., et al. 2011, *A&A*, 535, A33
- Muñoz, R. R., Geha, M., Côté, P., et al. 2012, *ApJ*, 753, L15
- Nishiyama, S., Tamura, M., Hatano, H., et al. 2009, *ApJ*, 696, 1407
- Ortolani, S., Barbuy, B., Bica, E., et al. 1999, *A&A*, 350, 840
- Ortolani, S., Bonatto, C., Bica, E., Barbuy, B., & Saito, R. K. 2012, *AJ*, 144, 147
- Pancino, E., Bellazzini, M., Giuffrida, G., & Marinoni, S. 2017, *MNRAS*, 467, 412
- Pedregosa, F., Varoquaux, G., Gramfort, A., et al. 2011, *Journal of Machine Learning Research*, 12, 2825
- Pérez, F. & Granger, B. E. 2007, *Computing in Science and Engineering*, 9, 21
- Reid, M. J. & Brunthaler, A. 2004, *ApJ*, 616, 872
- Riello, M., De Angeli, F., Evans, D. W., et al. 2018, *A&A*, 616, A3
- Ryu, J. & Lee, M. G. 2018, *ApJ*, 863, L38
- Surow, F., Valenti, E., Hidalgo, S. L., et al. 2019, *arXiv e-prints*
- Taylor, M. B. 2005, in *Astronomical Society of the Pacific Conference Series*, Vol. 347, *Astronomical Data Analysis Software and Systems XIV*, ed. P. Shopbell, M. Britton, & R. Ebert, 29
- Valcarce, A. A. R., Catelan, M., & De Medeiros, J. R. 2013, *A&A*, 553, A62
- van der Walt, Stéfan; Colbert, S. C. & Varoquaux, G. 2011, *Computing in Science and Engineering*, 13, 22
- Vasiliev, E. 2019, *MNRAS*, 484, 2832
- Webb, J. J. & Leigh, N. W. C. 2015, *MNRAS*, 453, 3278

Appendix A: Appendix

Diagnostic plots of the candidate globular clusters found in Gaia (left side) and VVV (right side). Each panel contains the sky position (upper left), VPD (lower left) and CMD (right) for the inner 1 arcmin (highlighted in orange) and the field stars within 10 arcmins from the nominal cluster center up to $G = 19$ mag. All the 93 candidate clusters but one (Minni 02) were located in the Gaia DR2 catalog and 53 in our VVV catalog. We recall that PMs are available from VVV only within latitudes $|b| < 3^\circ$, plus a few fields where they were calculated specifically for other projects.

